DOI: 10.15669/pnst.7.243

Progress in Nuclear Science and Technology
Volume 7 (2025) pp. 243-249

ARTICLE

Novel fiber reinforced concrete based on liquid metal technology toward resource recycling society

Masatoshi Kondo [a*], Yuki Kano [b], Nobuhiro Chijiwa [c] and Minho Oh [d]

[a] Laboratory for Zero-Carbon Energy, Institute of Integrated Research, Institute of Science Tokyo, Ookayama, Meguro-ku, Tokyo 152-8550, Japan [b] Graduate Major in Nuclear Engineering, Department of Mechanical Engineering, School of Engineering, Tokyo Institute of Technology, Ookayama, Meguro-ku, Tokyo 152-8550, Japan; [c] Department of Civil and Environmental Engineering, School of Environment and Society, Institute of Science Tokyo, Ookayama, Meguro-ku, Tokyo 152-8550 Japan; [d] Department of Materials Science and Engineering, School of Materials and Chemical Technology, Institute of Science Tokyo, Ookayama, Meguro-ku, Tokyo 152-8550, Japan

Conceptual study on recyclable reinforced concretes with low-melting-point metal fibers was carried out. The melting of reinforcing fibers by heating at low temperature enables the separation and recovery of fibers and cement from the FRC waste. Small beam test pieces of cement reinforced with staple shape fibers made of tin, aluminium and duralumin were fabricated. The results of three-point bending tests performed with the beam test pieces indicated that the failure resistance of cement was improved due to the reinforcement with the LMPM fibers. The removal of molten fibers from the cement matrix was demonstrated by means of model experiments using liquid GaInSn. The relocation behavior of liquid metal in narrow channel was clarified. Small chemical interaction of molten LMPMs with cement up to 1073 K was clarified by means of static immersion tests with cement specimens in the molten LMPMs.

Keywords: resource recycling; fiber-reinforced concrete; low-melting-point metal

1. Introduction

Concrete is one of the core materials for a human society, and cement is essential glue of the concrete. The global production of cement is greatly increasing mainly due to the economic growth of China and India as indicated in **Figure 1 (a)** [1], though the cement production keeps slight decrease in Japan. The global production of cement can reach 4.4 billion tons in 2050 according to the estimation in the cement technology roadmap [2]. Cement is produced by heating a mixture of clay, limestone and sand at around 1500°C. The emission of CO_2 involves in the cement production since limestone which is primarily calcium carbonates ($CaCO_3$) is decomposed into CaO and CO_2. The cement production also requires significant thermal energy to heat up the raw materials to a temperature around 1500°C, though the co-processing of industrial waste as a source of energy is reducing the use of fossil fuels [3]. The increase of the cement production (Figure 1(a)) cause the increase of global CO_2 emission as shown in **Figure 1 (b)** [4]. The global emission of CO_2 was approximately 34.7 Gt in 2015 [5]. Therefore, the CO_2 emission in the process of cement production corresponded to 4.2% of the total emission in 2015. The recycle of construction wastes is also essential for the reduction of environmental load. The waste concrete has been recycled as roadbed materials. However, the construction wastes mixed with metals and/or wood pieces are difficult to be recycled.

Fiber reinforced concrete or cement (FRC) has been developed, in which the toughness and structural integrity of concrete are reinforced by fibers of steel, glass, synthetic and natural [6]. The FRC has found many applications in a tunnel, a wall cladding, a bridge deck and pavement since the FRC can prevent a flaking and peeling of concrete due to its excellent resistance for the crack occurrence and propagation. However, the information on the recycle procedure of FRC after the service period is quite limited. The crushing process of FRC and the basic properties of crushed pieces were studied to clarify the recyclability of the FRC as aggregates and roadbed materials [7]. The crush of FRC can be conducted in the ordinary process by the use of a jaw crusher. The diameter of the crushed pieces was in a range between 2.5 mm to 50 mm. The fibers and mortar were separated when the FRC was crushed into small pieces which had a diameter in a range between 2.5 mm and 5 mm. However, the fibers were kept in large crushed pieces.

Fluids of low-melting-point metals (LMPMs) called as liquid metals are being applied as a coolant of nuclear fission and fusion reactors due to their excellent heat

*Corresponding author.
E-mail: kondou.m.fdb5@m.isct.ac.jp (Masatoshi Kondo)

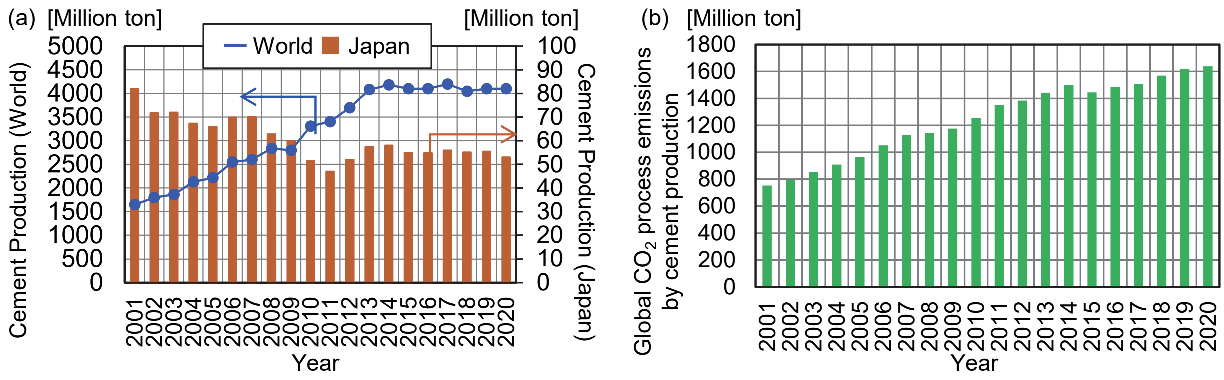

Figure 1. (a) Global cement production [Million ton] and cement production in Japan [Million ton] [1], (b) Global process emission by cement production [Million ton CO_2] [4].

transfer properties and neutron transport characteristics [8]. LMPMs have an inherent ability of solid-to-liquid phase change at their low melting points. The LMPMs reveals a rigidity in a solid state while the mobility of LMPMs is significantly promoted in a liquid state.

The purpose of the present study is to develop a recyclable FRC in which reinforcing fibers are made of low-melting-point metals. The LMPM fibers are separately recovered from the concrete matrix in a liquid state after the service period. Several prototypes of the LMPM FRC were fabricated, and their toughness was investigated by means of three-point bending tests with beam test pieces. The separation and recovery of LMPM fibers from the cement matrix in a liquid state was demonstrated by means of model experiments using liquid metal GaInSn. The chemical interaction between melting LMPM and cement matrix in the separation process at high temperature was also investigated by means of the compatibility tests.

2. Concept of LMPM FRC and its recycling procedure

Figure 2 shows the concept of LMPM FRC and its recycling procedure. The major features of the LMPM fibers are presented in **Table 1**. The cement or concrete matrix is reinforced by the random dispersion of the fibers made of the LMPM as described in the next chapter. The LMPM FRCs can be applied to the lining of tunnel and

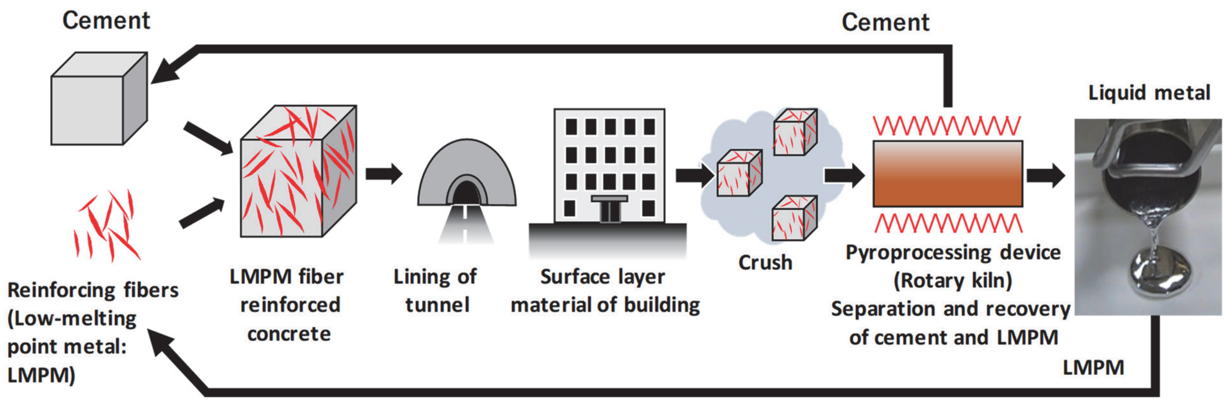

Figure 2. Concept of low-melting-point metal (LMPM) fiber reinforced concrete (FRC) and its recycling procedure.

Table 1. Major properties of LMPM and their fibers

	Fibers		Liquid metals		
	Young's modulus [GPa]	Tensile stress [GPa]	Melting point [K]	Density [kg/m^3]	Viscosity [mPas]
Tin (Sn)	50	30	505.1	6902 at 600 K	1.56 at 600 K
Aluminum (Al)	70	100	933.5	2353 at 1000K	2.5 at 1000 K
Duralumin (A2017)	70	355	933.6	Similar to Al	Similar to Al
GaInSn	-	-	527.2	6440 at 293 K	2.09 at 299 K
Steel (S45C) (reference)	205	828	1808.2	-	-
Glass (reference)	70	>2000	1673.2	-	-

the surface layer material of buildings in the same way to the conventional FRCs. The LMPM FRC is crushed into small pieces after the service period. The crushed pieces are heated to a temperature higher than the melting point of LMPMs and the melted LMPM fibers are physically removed from the FRC matrix by an external force such as a centrifugal force. This recovery process can be performed in a pyroprocessing device similar to a rotary kiln used for the cement production (i.e. 1500°C), though the operation temperature in the recovery process is much lower than that required for the cement production. The LMPM and cement are separately recovered and recycled. The cementitious powder of waste concrete is recycled as raw material of cement as a substitute for limestone [9], and the recycle can contribute the reduction of CO_2 emission in the process of cement production [10].

3. Three-point bending tests with beam test pieces of LMPM FRC fabricated

Some prototypes of FRC were designed with the LMPM fibers of tin (Sn, purity: 99.9 wt%), aluminum (Al, purity: 99.99 wt%) and duralumin (A2017, Al-3.82Cu-0.6Mg-0.45Si-0.54Mn-0.23Fe-0.01Cr-0.06Zn-0.03Ti in wt%). The mechanical properties of the LMPM fibers is inferior than those of steel and glass fibers as presented in Table 1, though the melting point of the LMPM fibers is much lower than that of steels. The LMPM FRC were fabricated with an ordinary Portland cement (OPC) and LMPM fibers which had a staple geometry as shown in **Figure 3 (a)**. The chemical composition of OPC is presented in **Table 2**. The water-cement (W/C) ratio of LMPM FRC was 35 wt% due to the need of viscosity to control material segregation. The diameter of the fibers was 2 mm. The volumetric ratio of the LMPM fibers was in a range between 1 - 5 vol% as shown in **Table 3**. Three-point bending tests were performed with the beam test pieces which had a size of 40 mm × 40 mm × 160 mm as shown in **Figure 3 (b)**. All the test pieces were set and cured in water at room temperature for 14 days.

The three-point bending tests were performed at a clear span of 150 mm as shown in **Figure 3 (c)** under a constant displacement control of 0.2 mm/min. **Figure 4** shows the load- displacement curves (LDCs) obtained by the three-point bending tests. The failure of the plane cement test piece PL35 was caused when the displacement reached approximately 0.5mm and the load reached approximately 1200 N as shown in **Figure 4 (a)**. The FRC test piece of

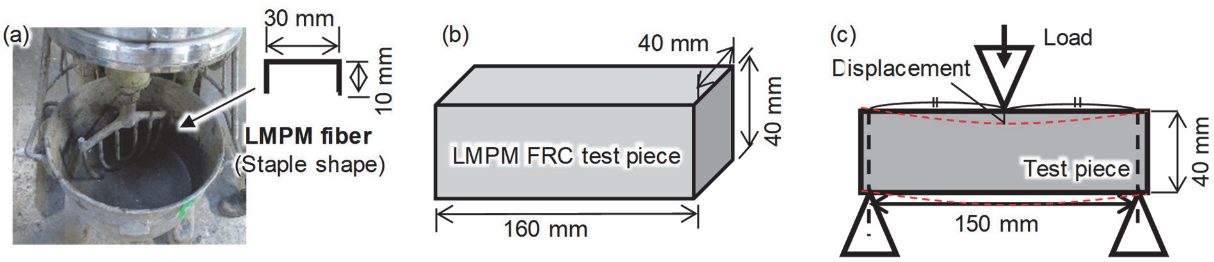

Figure 3. (a) Fabrication of LMPM FRC, (b) Beam test pieces of LMPM FRCs (40 mm × 40 mm ×160 mm), (c) Three-point bending test.

Table 2. Chemical composition of ordinary Portland cement (OPC) [wt%].

C_3S ($3CaO \cdot SiO_2$)	C_2S ($2CaO \cdot SiO_2$)	C_3A ($3CaO \cdot Al_2O_3$)	C_4AF ($4CaO \cdot Al_2O_3 \cdot Fe_2O_3$)	MgO	SO_3	Cl^-	Na_2Oeq
56	18	9	9	1.41	2.1	0.015	0.5

Table 3. Beam test pieces fabricated for three-point bending tests.

Test ID	W/C* [%]	Fiber material	Fiber diameter [mm]	Fiber Length [mm]	Fiber Shape	Fiber amount [vol%]
S2-1	35	Sn (99.99 %)	2.0	30	Staple	1.0
S2-2	35	Sn (99.99 %)	2.0	30	Staple	2.0
S2-5	35	Sn (99.99 %)	2.0	30	Staple	5.0
A2-1	35	Al (99.99 %)	2.0	30	Staple	1.0
A2-2	35	Al (99.99 %)	2.0	30	Staple	2.0
A2-5	35	Al (99.99 %)	2.0	30	Staple	5.0
D2-1	35	Duralumin (A2017)	2.0	30	Staple	1.0
D2-2	35	Duralumin (A2017)	2.0	30	Staple	2.0
D2-5	35	Duralumin (A2017)	2.0	30	Staple	5.0
PL35	35	No fibers	—	—	—	0

*(Water[g]/Cement[g]=W/C)

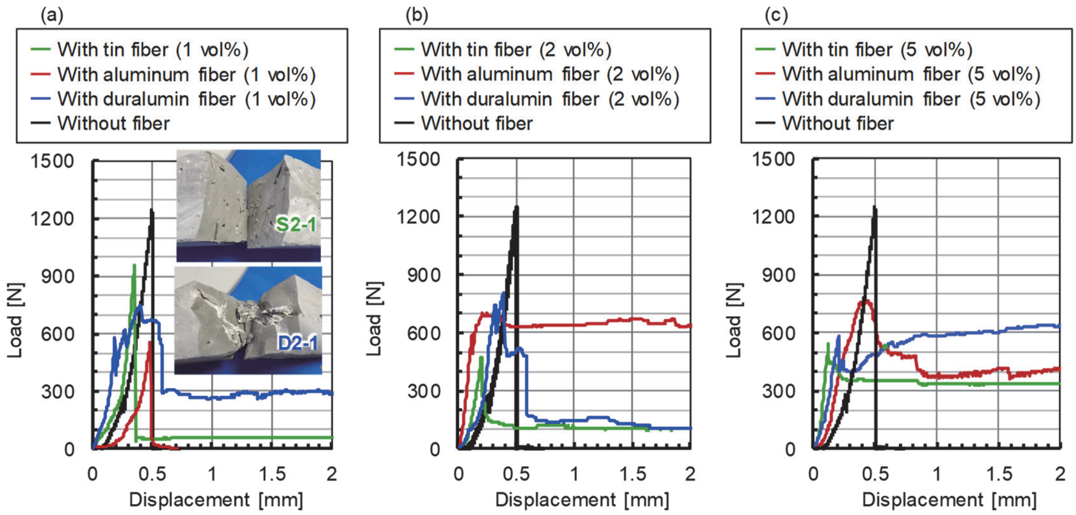

Figure 4. (a) Load-displacement curves obtained by three-point bending tests with LMPM FRC beam test pieces having a size of 40 mm × 40 mm × 160 mm (1) 1 vol% LMPM fibers, (b) 2 vol% LMPM fibers and (c) 5 vol% LMPM fibers.

D2-1 revealed the larger displacement until the failure, though those of S2-1 and A2-1 did not clearly reveal the improvement. The fracture surface of S2-1 and A2-1 test pieces was relatively flat as the same as that of PL35, and the failure of the fibers without the pull out was also recognized. The facture surface of D2-1 was irregular and the pull out of the fibers was recognized. **Figures 4 (b) and (c)** show the LDCs obtained with the test pieces including 2 vol% and 5 vol% LMPM fibers, respectively. The test pieces of FRC with Sn fibers revealed the larger displacement until the failure when the content of fiber volume was larger than 2 vol%. The displacement until the failure was significantly larger in the all LMPM FRCs when the fiber volume content was 5 vol%. The diameter of LMPM fibers was 2 mm and larger rather than the ordinary FRCs. The number density of fibers was small especially in the FRC test pieces in which the fiber content was 1 vol%. The crack extension and/or propagation for the failure could not be suppressed when the fibers were not located around the crack. Therefore, the failure behaviors of the test pieces could be influenced by the arrangement of fibers when the number density of fibers was small. The failure resistance of the LMPM FRC was promoted when the fiber arrangement was improved according to the increase of fiber volume content. However, the fluidity and workability of cement slurry is lower when the fiber content is higher. The LDCs of all the LMPM FRCs indicated that their peak flexural load was lower than that of plane cement. The flexural strength was reduced by the dispersion of fibers possibly since the initial crack occurrence could be induced around the fibers in the test pieces.

4. Separation and recovery of molten LMPM fibers from cement matrix

Figure 5 (a) schematically illustrates the separation and recovery of molten LMPM fibers from small crushed pieces of waste LMPM FRCs. The crushed pieces are heated to a temperature higher than the melting point of LMPM in a pyroprocess device as explained in Figure 1. The fibers are expected to be remained in the crushed pieces as they expose their both edges or only one edge. The removal of melting LMPM fiber from the FRC matrix by centrifugal force is demonstrated by means of the model experiments as shown in **Figure 5 (b)**. Liquid metal GaInSn was used as a simulant fluid, since the fluid properties of liquid GaInSn are similar with those of LMPMs [11]. Liquid GaInSn was installed in the slender tube which had an inner diameter of 3 mm. Liquid GaInSn of 1.4 cc was installed in the tube when the both ends of the tube were opened, and that of 0.7 cc was installed in the tube when the one end was closed. The length of liquid GaInSn was 10 cm. The tube was rotated around the shaft at a rotational speed in a range between 30 and 150 rpm. The arrangement of fibers in crushed pieces can be changed due to the mixing of the crushed pieces in a pyroprocess device. Therefore, the holding angle of the tube from a horizontal plane was varied in a range between 0 ° and 30 ° to simulate the various arrangement of fibers in the recovery process. The forces working on liquid GaInSn are shown in **Figure 5 (a)**. Liquid GaInSn bulk slowly relocates in the tube to the radial outside and escapes from the edge of the tube as shown in **Figure 5 (c)**, when the centrifugal force is larger than the sum of gravity force, viscous resistance and surface tension. The recovery ratio of liquid GaInSn was evaluated by the measurement of liquid GaInSn removed from the tube after the recovery experiments performed for 5 minutes. The liquid metal did not relocate at all in the tube when the centrifugal force worked on the liquid metal bulk was smaller the sum of other resistance forces. However, the time required for the removal of liquid metal from the tube was within 3 minutes when the liquid metal could relocate in the tube with the centrifugal force larger than the sum of other resistance forces. Therefore, current recovery duration (i.e.

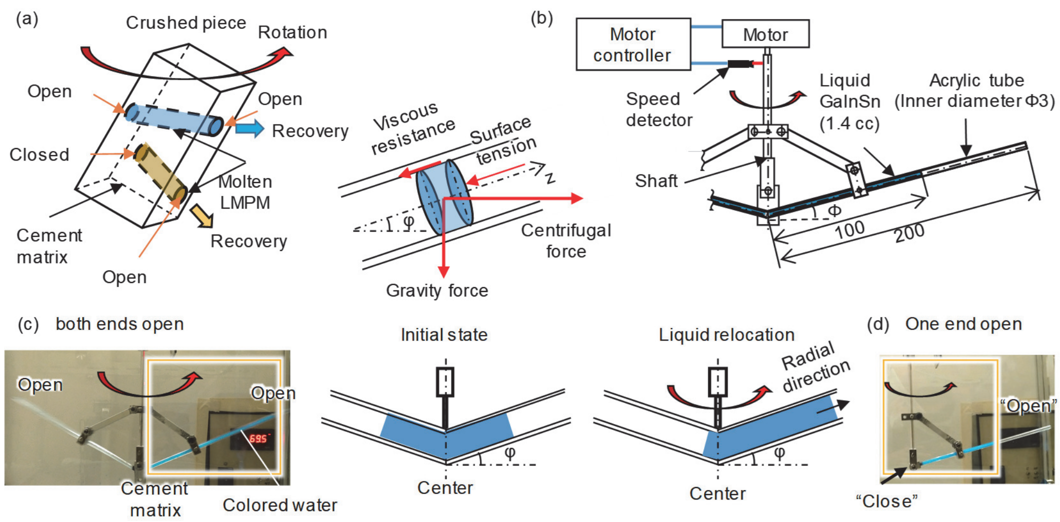

Figure 5. (a) Removal of melting LMPM fibers from crushed pieces of FRC waste, (b) experimental apparatus for liquid metal recovery from slender acrylic tube by centrifugal force, (c) Liquid relocation in tube open at both ends, (d) Tube closed at one end and open at other end.

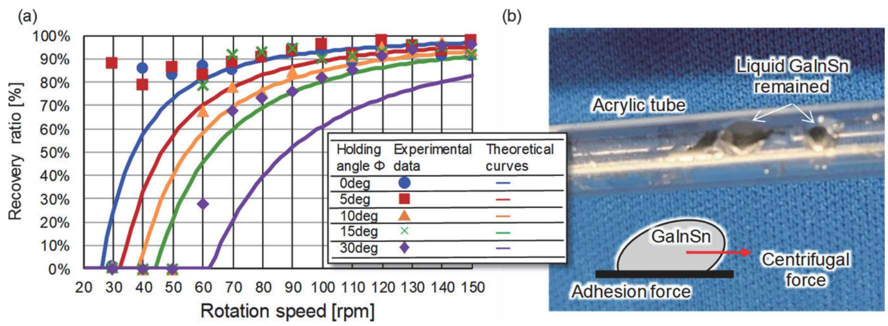

Figure 6. (a) Results of recovery experiments with liquid GaInSn, (b) Liquid GaInSn droplet remained in acrylic tube.

5 minutes) was sufficiently long to evaluate the recovery ratio.

Figure 6 (a) shows the recovery ratio of liquid GaInSn in the experiment, in which both ends of the slender tube were opened. The plots indicate the experimental data and the solid lines indicate the theoretical curves based on the estimation of resultant force worked on the liquid bulk. Liquid GaInSn could be removed at lower rotational speed when the holding angle was smaller. The increase of the rotational speed promoted the recovery ratio even when the holding angle was small. Liquid GaInSn could not be removed at the rotational speed lower than 50 rpm when the holding angle was larger than 10 °. The trends of experimental data and the theoretical curves clearly indicated that there were threshold values of centrifugal force necessary for the recovery of liquid metal when the holding angle was larger than 10 °. The force necessary for the liquid relocation in the tube and the release from the tube end was roughly estimated as 3 N/kg in the present geometry. This magnitude of centrifugal force can be achieved by ordinary rotary kilns which have a diameter of 6 m and a rotational speed of 10 rpm. Some small droplets of liquid GaInSn remained in the acrylic tube after the recovery experiments as shown in **Figure 6 (b)**, which could be formed in the tube due to the large surface tension of liquid GaInSn. They did not relocate radially to the outside of the tube since the centrifugal force worked on the small drop was smaller than its adhesion force between the droplet and the acrylic wall. Liquid GaInSn could not be recovered in the experiments when the one end of tube was opened and the other end was closed as shown in **Figure 5 (d)**. Liquid GaInSn bulk could not be relocated to the radial direction in the tube since an atmospheric pressure worked on the liquid bulk.

5. Chemical interaction between molten LMPM and cement matrix

The chemical interaction between molten LMPMs (i.e. Sn, Al and duralumin (A2017)) and cement matrix was investigated by means of static immersion tests [8]. The rectangular specimen of plane cement (W/C=35 %) which had a size of 10 mm × 15 mm × 4 mm was installed with LMPM of 3 cc in the crucible made of 316 L austenitic steel (Fe-18Cr-12Ni-2Mo) as shown in **Figure 7 (a)**. This LMPM test assemble was installed in the test vessel filled with high purity Ar (99.99%). The immersion test in liquid Sn was performed at 773K, and those in liquid Al and duralumin were performed at 1073 K. The test duration was 250 hours. Molten LMPM fiber can be recovered from the concrete waste within several minutes according to the results of recovery experiments as described in the previous chapter. Therefore, the test duration of the immersion tests was much larger than the time necessary for the separation and recovery of molten LMPM fibers.

The cement specimens were exposed to Ar atmosphere at 773 K and 1073 K to clarify the effect of heat treatment on the cement characteristics at the test temperatures.

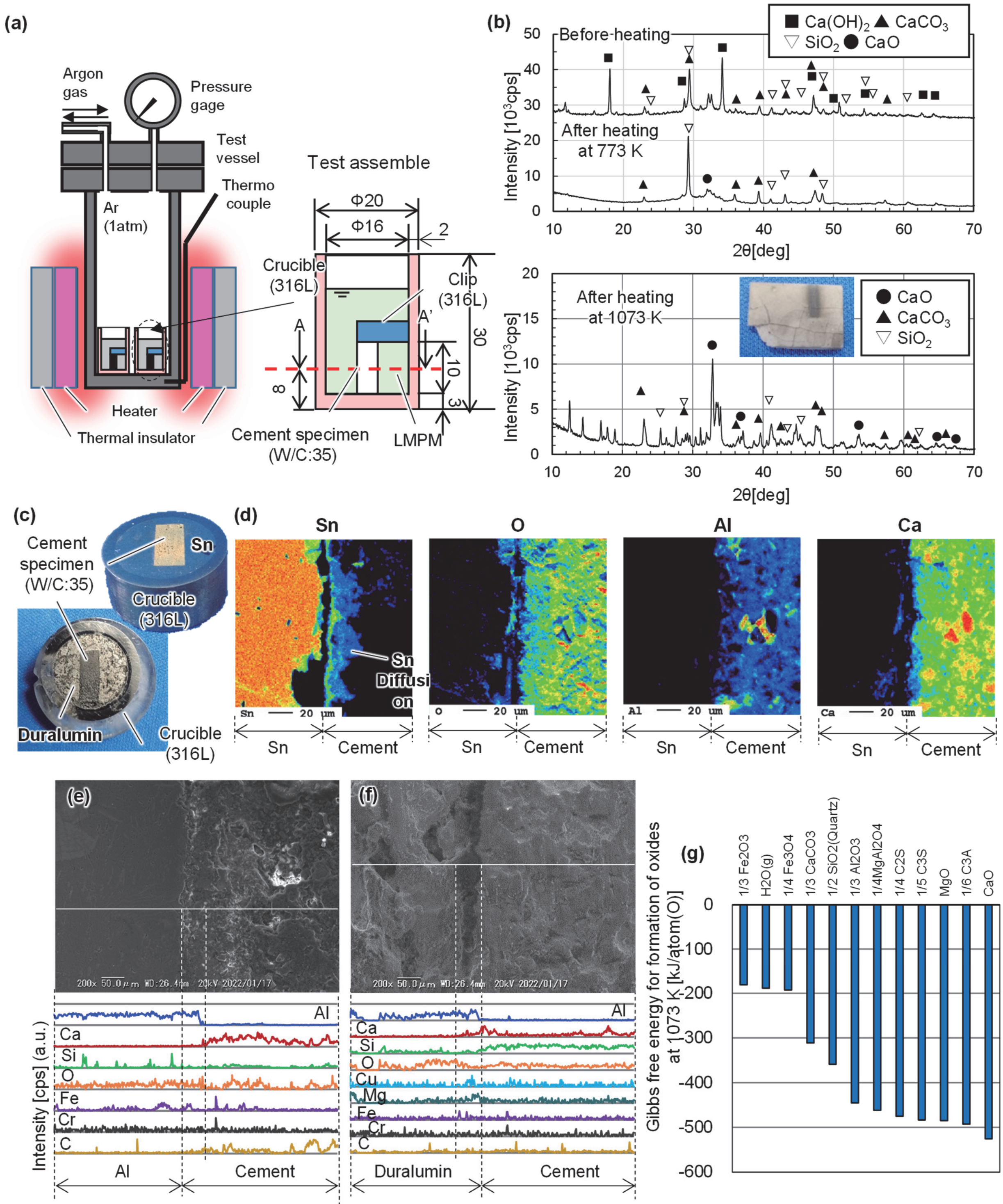

Figure 7. (a) Compatibility test assemble, (b) XRD analysis on cement after exposure to high temperature Ar, (c) cross sectional photo images of test assembles after compatibility tests with Sn and duralumin, (d) Cross sectional EPMA analysis on cement specimen exposed to liquid Sn at 773 K, (e) the cross sectional SEM/EDX analysis on cement specimen exposed to liquid Al, (f) the cross sectional SEM/EDX analysis on cement specimen exposed to liquid duralumin and (g) Gibbs free energy for formation of oxides at 1073 K.

Figure 7 (b) shows the results of XRD analysis on the specimens after the heat treatment. $Ca(OH)_2$ decomposed into CaO and H_2O, and the decomposition was more significant at higher temperature. The LMPM test assembles were horizontally cut at the position of A-A' after the tests. The cross sections were shown in **Figure 7 (c)**. The cross section of the cement specimen was observed and analyzed by a scanning electron microscope (SEM) with an energy dispersive X-ray spectroscopy (EDX) and an electron probe micro analyzer (EPMA). The slight diffusion of Sn into cement matrix was detected and the depth was approximately 20 μm as shown in **Figure 7 (d)**. **Figure 7 (e)** shows the result of cross sectional SEM/EDX analysis on the cement specimen exposed to liquid Al at 1073 K. The diffusion of Al into cement matrix was detected, and the depth was approximately 50 μm. **Figure 7 (f)** shows the result of cross sectional SEM/EDX analysis on the cement specimen exposed to liquid duralumin. The elements of cement composition (i.e. Ca, Si and O) might diffuse into molten duralumin. **Figure 7 (g)** shows the Gibbs free energy for the formation of oxides. The chemical interaction between the LMPMs and the cement was not so remarkable since the cement compositions are thermodynamically stable rather than the oxides of LMPMs.

4. Conclusion

Conceptual study on recyclable concretes reinforced with the LMPM fibers was carried out. The three-point bending tests were performed with the small beam test pieces (40 mm × 40 mm × 160 mm) of LMPM FRCs. The resistance for the failure was improved by the reinforcement with the LMPM fibers. The separation and recovery process of molten LMPM fibers from FRC waste was experimentally studied by means of model experiments using liquid GaInSn. Liquid GaInSn relocated in the narrow channel which had an inner diameter of 3mm according to a centrifugal force. The chemical interaction between liquid LMPMs, and the cement was negligibly small. The collective results motivate a sustainable management of FRC waste, which promotes a sustainable society through the low melting point metal technologies.

Acknowledgements

This research was financially supported by Interdisciplinary Research Support for Scientists of Tokyo Institute of Technology.

References

[1] U.S. Geological Survey, Mineral commodity summaries 2000 ~ 2021: U.S. Geological Survey.
[2] IEA, Cement Technology Roadmap: Carbon Emissions Reductions up to 2050, IEA Technology Roadmaps, (2009), OECD Publishing.
[3] W. de Queiroz Lamas, J.C and Fortes Palau, J.R. de Camargo, Waste materials co-processing in cement industry: Ecological efficiency of waste reuse, *Renewable and Sustainable Energy Reviews* 19 (2013), pp. 200-207.
[4] A. Robbie. Global CO2 emissions from cement production (Version 220516) [Data set] (2022), Zenodo.
[5] IEA, CO2 Emissions in 2022, IEA, Paris, (2023).
[6] R.F. Zollo, Fiber-reinforced concrete: an overview after 30 years of development, *Cement and Concrete Composites* 19 (1997), pp. 107-122.
[7] M. Kunieda, N. Ueda and H. Nakamura, Ability of recycling on fiber reinforced concrete, *Construction and Building Materials*, 67, Part C (2014), pp. 315-320.
[8] M. Kondo, S. Hatakeyama, N. Oono and T. Nozawa, Corrosion-resistant materials for liquid LiPb fusion blanket in elevated temperature operation, *Corrosion Science* 197 (2022), 110070.
[9] K. Eunhee, J. Ahn, B. Cho and D. Park, A study on development of recycled cement made from waste cementitious powder, *Construction and Building Materials* 83 (2015), pp. 174-180.
[10] O. Da-Young, T. Noguchi, R. Kitagaki and W-J. Park, CO_2 emission reduction by reuse of building material waste in the Japanese cement industry, *Renewable and Sustainable Energy Reviews* 38 (2014), pp. 796-810.
[11] L. Battezzati and A.L. Greer, The viscosity of liquid metals and alloys, *Acta Metallurgica* 37 (1989), pp. 1791-1802.